

A comparative study of sol-gel synthesized ZnO/GO and ZnO/g-C₃N₄ nanocomposites in the photocatalytic degradation of acetaminophen

Judith Chebwogen^{1,2}, Francis W. Nyongesa², Julius M. Mwabora², Gershom M. Ntshani¹,
and Patrick G. Ndungu^{1*}

¹Department of Chemistry, University of Pretoria, Private Bag X20, Hartfield, 0028, South Africa

²Department of Physics, University of Nairobi, P.O. Box 30197-00100, Nairobi, Kenya.

*Corresponding author email: patrick.ndungu@up.ac.za

UV-A lamp emission spectrum

The emission spectrum of the commercial UV-A lamp used in this work was measured using an Avantes spectrometer (AvaSpec-ULS3648 StarLine High-resolution Fiber-optic Spectrometer) that employs an optical fiber to transmit light to its diffraction grating. An absorptive neutral density filter (NE06B-A - 0.6 OD with range 350 to 700 nm) from Thorlabs was used to prevent detector saturation. **Figure S1** shows the spectrum obtained.

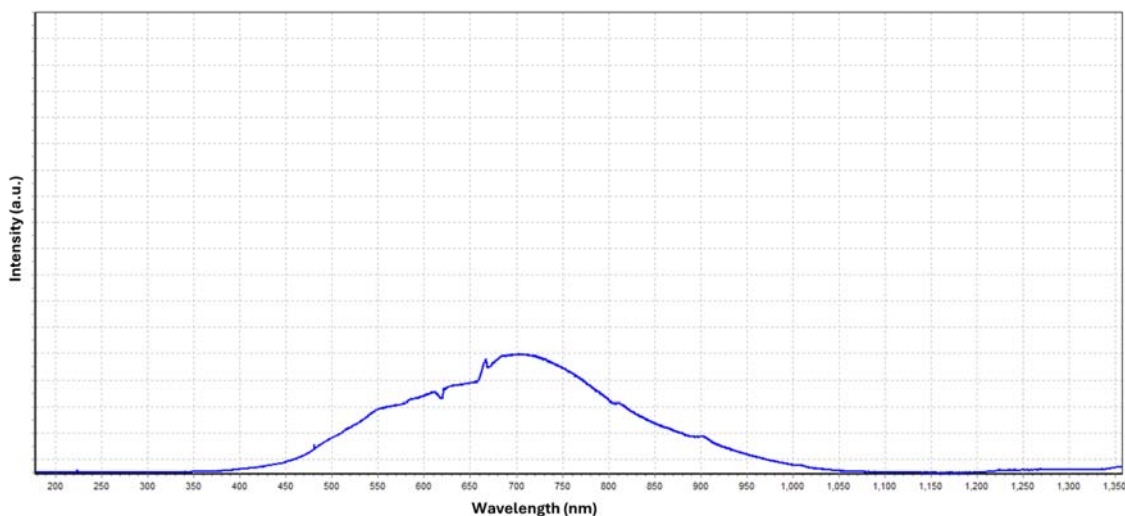


Figure S1: Measured UV-A lamp light emission spectrum

Crystal size and lattice parameters determination

Peaks with the greatest intensity in the diffractograms obtained were used to calculate the crystal size using the Debye-Scherrer relation (Scherrer, 1918):

$$D = \frac{k\lambda}{\beta \cos\theta} \quad (\text{Equation S1})$$

Where $K=0.9$, $\lambda= 1.5406 \text{ \AA}$, β is the width of the peak and θ is half the peak location angle.

Equations 2 and **3** were used to determine lattice constants 'a' and 'c' since ZnO has a hexagonal unit cell with two lattice parameters 'a' and 'c' (Lupan et al., 2010). The lattice parameters aided the calculation of the interplanar distance using **Equation 4** and the unit cell volume using **Equation 5** (Bhosale et al., 2023).

$$a = \frac{\lambda}{\sqrt{3}\sin\theta} \quad (\text{Equation S2})$$

$$c = \frac{\lambda}{\sin\theta} \quad (\text{Equation S3})$$

$$\frac{1}{d^2} = \frac{4}{3} \left(\frac{h^2+hk+k^2}{a^2} \right) + \frac{l^2}{c^2} \quad (\text{Equation S4})$$

$$V = \frac{\sqrt{3}}{2} a^2 \cdot c \quad (\text{Equation S5})$$

Where a and c are lattice parameters, λ is X-ray wavelength (1.5406 \AA), θ is half the peak angle, (hkl) are miller indices, d is the interplanar distance and V is the unit cell volume.

TGA curves

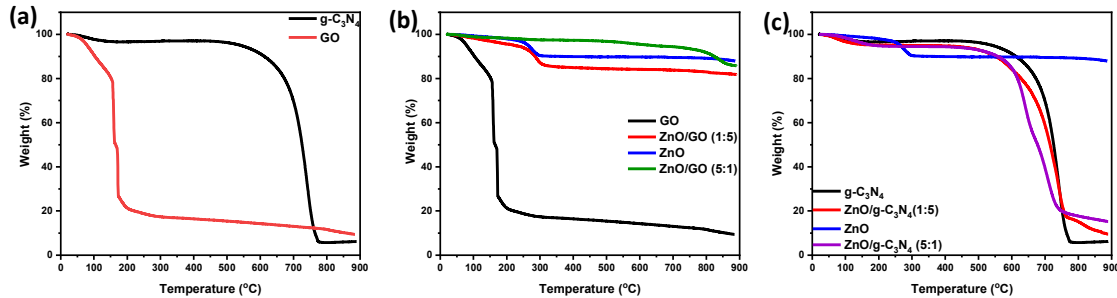


Figure S2: Thermal properties of g-C₃N₄ and GO (a), ZnO, GO and their nanocomposites (b), ZnO, g-C₃N₄ and their nanocomposites

Pore size distribution curves

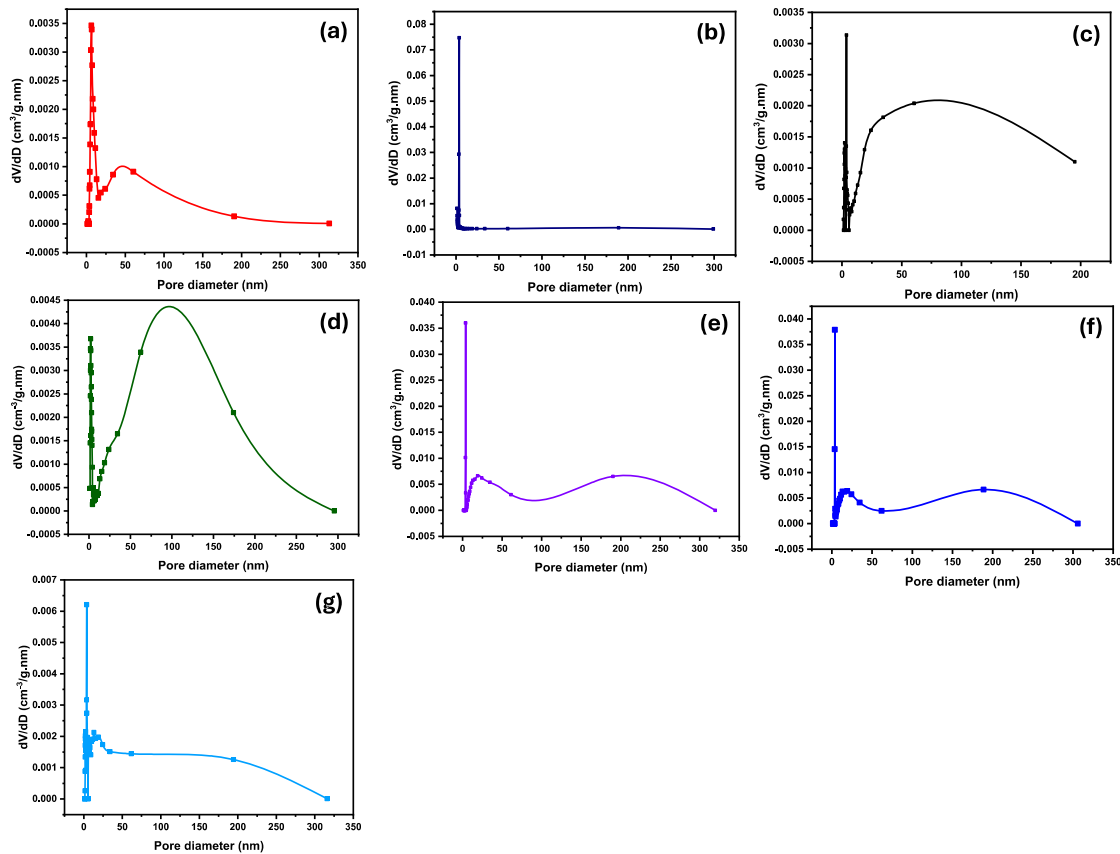


Figure S3: Pore size distribution graphs for ZnO (a), GO (b), ZnO/GO (1:5) (c), ZnO/GO (5:1) (d), g-C₃N₄ (e), ZnO/g-C₃N₄ (1:5) (f) and ZnO/g-C₃N₄ (5:1) (g)

Proposed acetaminophen degradation pathways

A mass spectrometer was applied to characterize various acetaminophen degradation intermediates in the presence of the photocatalysts. Throughout the analysis, it was observed that hydroxyl radicals played a major role. Acetaminophen mineralization may have taken place through three mechanisms where the hydroxide radical attacked either the phenyl ring on the ortho or para position with respect to the hydroxyl group, or the acetamide on the C=O carbon (Moctezuma et al., 2012). These mechanisms were confirmed by the detection of various structural intermediates. The hydroxyl group is an ortho-para directing activator with equal chances on both ortho and para positions. The first mechanism (M1) shows an attack of the •OH radical on the ortho position with respect to the hydroxyl functional group which was

confirmed by the $m/z = 167$ of the hydroxylated acetaminophen (Le et al., 2021). The $m/z = 167$ confirmed that the acetamide was still attached to the ring as opposed to the attack on the para position which forms a radical that can immediately cleave the acetamide group. The second mechanism (M2) involves the attachment of the hydroxyl on the para position with respect to the hydroxyl group. This pathway was confirmed by the presence of the quinol at $m/z = 110$ (Nasr et al., 2019).

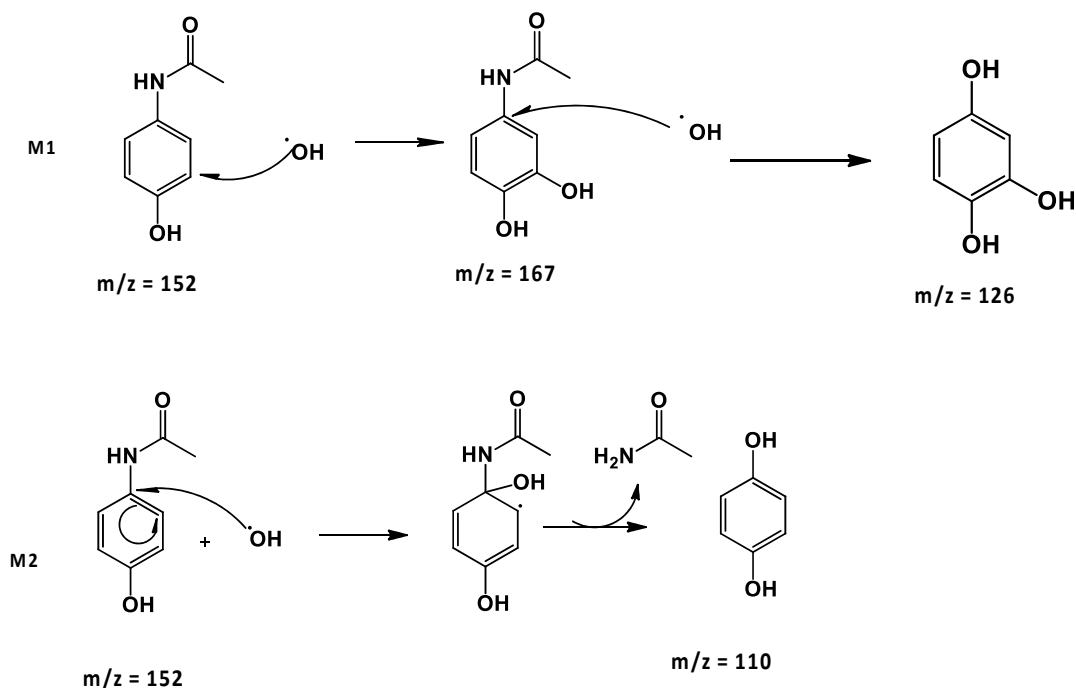


Figure S4: Proposed acetaminophen photodegradation pathways

Acetaminophen photodegradation mechanisms

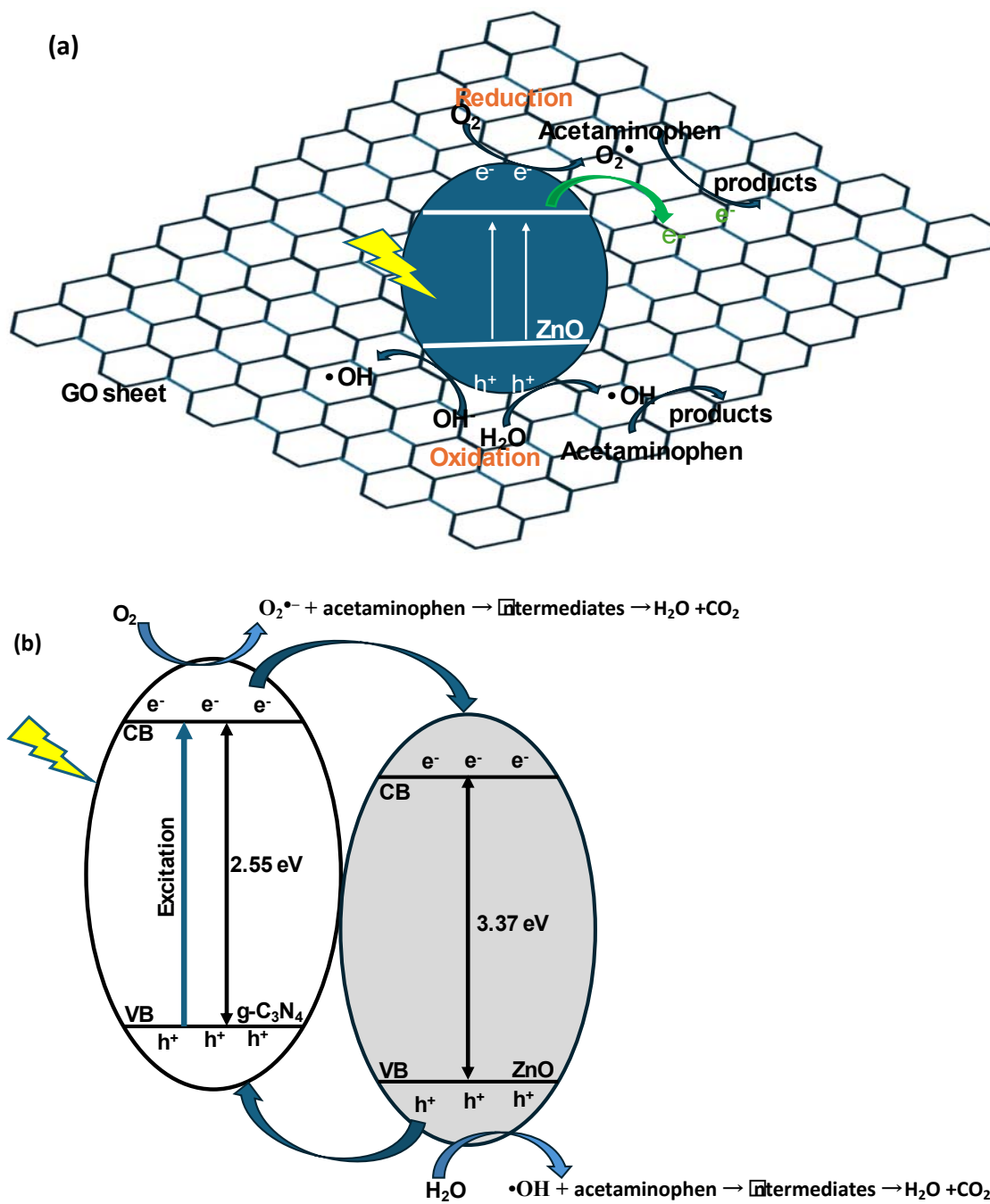


Figure S5: Photodegradation mechanisms of ZnO/GO (a) and ZnO/g-C₃N₄ (b)

References

- Bhosale, A., Gophane, A., Kadam, J., Sabale, S., Sonawane, K., & Garadkar, K. (2023). Fabrication of visible-active ZnO-gC₃N₄ nanocomposites for photodegradation and cytotoxicity of methyl orange and antibacterial activity towards drug resistance pathogens. *Optical Materials*, 136, 113392. <https://doi.org/https://doi.org/10.1016/j.optmat.2022.113392>
- Le, T. X. H., Nguyen, T. V. A., Zoukifli, A. Y., Zoungrana, L., Avril, F., Nguyen, D. L., Petit, E., Mendret, J., Bonniol, V., Bechelany, Lacour, S., Lesage, G., & Cretin, M. (2021). Degradation pathway and toxicity of acetaminophen by electro-Fenton processes in 1 aqueous media 2 3.
- Lupan, O., Pauporté, T., Chow, L., Viana, B., Pellé, F., Ono, L. K., Roldan Cuenya, B., & Heinrich, H. (2010). Effects of annealing on properties of ZnO thin films prepared by electrochemical deposition in chloride medium. *Applied Surface Science*, 256(6), 1895-1907. <https://doi.org/https://doi.org/10.1016/j.apsusc.2009.10.032>
- Moctezuma, E., Leyva, E., Aguilar, C. A., Luna, R. A., & Montalvo, C. (2012). Photocatalytic degradation of paracetamol: Intermediates and total reaction mechanism. *Journal of Hazardous Materials*, 243, 130-138. <https://doi.org/https://doi.org/10.1016/j.jhazmat.2012.10.010>
- Nasr, O., Mohamed, O., Al-Shirbini, A.-S., & Abdel-Wahab, A.-M. (2019). Photocatalytic degradation of acetaminophen over Ag, Au and Pt loaded TiO₂ using solar light. *Journal of Photochemistry and Photobiology A: Chemistry*, 374, 185-193. <https://doi.org/https://doi.org/10.1016/j.jphotochem.2019.01.032>
- Scherrer, P. (1918). Bestimmung der Grosse und inneren Struktur von Kolloidteilchen mittels Rontgenstrahlen. *Nach Ges Wiss Gottingen*, 2, 8-100.